IOPscience iopscience.iop.org

Home Search Collections Journals About Contact us My IOPscience

A high power InGaAs/GaAsP vertical-cavity surface-emitting laser and its temperature characteristics

This article has been downloaded from IOPscience. Please scroll down to see the full text article.

2004 Semicond. Sci. Technol. 19 685

(http://iopscience.iop.org/0268-1242/19/6/004)

View the table of contents for this issue, or go to the journal homepage for more

Download details:
IP Address: 159.226.165.151
The article was downloaded on 05/09/2012 at 04:45

Please note that terms and conditions apply.

Semicond. Sci. Technol. **19** (2004) 685–689 PII: S0268-1242(04)69941-X

# A high power InGaAs/GaAsP vertical-cavity surface-emitting laser and its temperature characteristics

**Changling Yan[1,2], Yongqiang Ning[1], Li Qin[1], Shumin Zhang[3], Qing Wang[1], Lumin Zhao[1], Zhenhua Jin[1], Yanfang Sun[1], Getao Tao[1], Yun Liu[1], Guoqiang Chu[1], Lijun Wang[1] and Huilin Jiang[2]**

[1] Laboratory of Excited State Processes, Changchun Institute of Optics, Fine Mechanics and Physics, Chinese Academy of Sciences, Changchun 130021, People's Republic of China
[2] State Key Laboratory of High-Power Semiconductor Lasers, Changchun University of Science and Technology, Changchun 130022, People's Republic of China
[3] Jilin University, Changchun, 130023, People's Republic of China

E-mail: changling_yan@yahoo.com.cn

Received 5 October 2003
Published 8 April 2004
Online at stacks.iop.org/SST/19/685 (DOI: 10.1088/0268-1242/19/6/004)

**Abstract**
A high power bottom-emitting InGaAs/GaAsP vertical-cavity surface-emitting laser with a large aperture (400 $\mu$m diameter) is described. The device has been fabricated by using oxidation confinement technology. The device threshold current is 610 mA, and the maximum output power is up to the watt regime (1.42 W) at room temperature (24 °C) with a pulse condition (pulse width of 50 $\mu$s, repetition rate of 1 kHz). The maximum continuous wave optical output power at room temperature is as high as 1.09 W. The lasing peak wavelength is 987 nm, the full width at half-maximum is 0.9 nm, and the far-field divergence angle is below 10°. The temperature characteristics of the device are also obtained. A special temperature dependence of the threshold current in the vertical-cavity surface-emitting laser structure is observed; the characteristic temperature $T_0$ is over 220 K, and the wavelength shift with temperature is only about 0.06 nm $K^{-1}$.

## 1. Introduction

Due to the attractive features of the vertical emitting geometry, vertical-cavity surface-emitting lasers (VCSELs) have shown many advantages over conventional edge-emitting lasers, such as a circular light-output mode, a high packing density for two-dimensional arrays and single longitudinal mode emission due to the inherent short cavity length [1–3]. In particular, the AlAs oxide confinement technology is so successfully used in device fabrication that VCSEL devices have been used in many applications [4]. Low power VCSELs with small-diameter apertures (less than 20 $\mu$m) are greatly desired for such applications as optical imaging, scanning, and massive parallel optical interconnects [5–7]. The applications in free space communication, laser pumping, medicine, and materials treatment are revealing a growing market for high power diode lasers [8–10], so it should be valuable to work out the potentialities of VCSELs for high power applications. In particular, high power spatially incoherent diode lasers with narrow spectral widths in the 940–980 nm wavelength range are desirable for pumping solid-state lasers and instrumentation applications [11, 12]. The highest optical output power level reported for a single device is from the CW optical power 0.89 W VCSEL with InGaAs/GaAs QWs [13, 14]. In this paper we report a high power bottom-emitting InGaAs/GaAsP VCSEL with a large aperture (400 $\mu$m diameter) at about 980 nm wavelength. Oxidation confinement technology is used in the device fabrication process to form the current aperture and determine the active diameter of the device. The performance characteristics, such as the threshold condition, output power, laser spectrum, and far-field pattern, are

© 2004 IOP Publishing Ltd Printed in the UK 

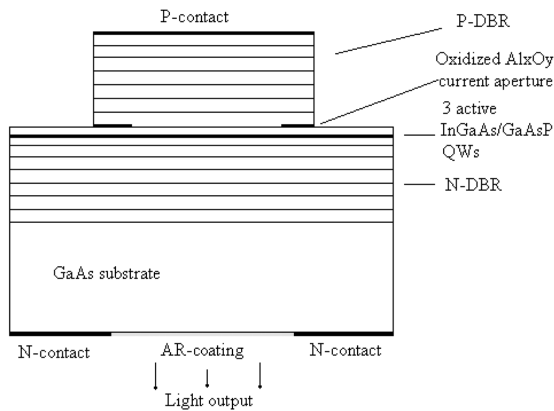


**Figure 1.** A schematic diagram of the device structure.

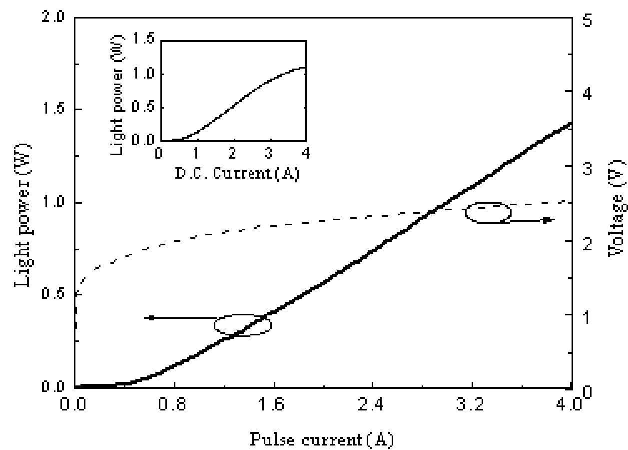


**Figure 2.** Measured output characteristics of the device; the inset shows the measured CW optical output characteristic.

obtained experimentally at room temperature (24 °C). Both the pulse condition and the continuous wave (CW) maximum optical output power are up to the watt regime, the full width at half-maximum of the lasing spectrum is 0.9 nm, and the far-field divergence is below 10°. The temperature characteristics of the device are also obtained.

## 2. Device structure

The structure of the bottom-emitting device is shown in figure 1. The inner cavity contains three 6 nm thick $In_{0.2}Ga_{0.8}As$ quantum wells embedded in 8 nm thick $GaAs_{0.92}P_{0.08}$ barriers. $Al_xGa_{1-x}As$ cladding layers are used to form a 1 $\lambda$ cavity. The carbon-doped p-type distributed Bragg reflector consists of 35.5 $Al_{0.9}Ga_{0.1}As/Al_{0.12}Ga_{0.88}As$ pairs with graded interfaces to reduce the series resistance. The top 100 nm GaAs contact layer is doped to a concentration of $1 \times 10^{19}$ cm$^{-3}$ to achieve a good ohmic contact. There is a 30 nm thick $Al_{0.98}Ga_{0.02}As$ layer located between the active region and the top p-type mirror. This layer is oxidized and converted to $Al_xO_y$ later in the fabrication process for current confinement and determining the active diameter of the device. The silicon-doped n-type distributed Bragg reflector (DBR) has only 25.5 $Al_{0.9}Ga_{0.1}As/Al_{0.12}Ga_{0.88}As$ pairs for light bottom emission through the GaAs substrate. The device structure layers are grown on a (100) GaAs substrate by using low pressure metal–organic chemical vapour deposition (MOCVD). The group-V precursors are the hydride sources $AsH_3$ and $PH_3$. The group-III precursors are trimethyl alkyls of gallium (Ga), aluminium (Al), and indium (In) respectively. The $Al_{0.9}Ga_{0.1}As/Al_{0.12}Ga_{0.88}As$ DBRs are grown at about 750 °C, and the three-quantum-well active region growth temperature is selected to be about 650 °C.

Wet chemical etching is used to define a circular mesa; the etch reaches the $Al_{0.98}Ga_{0.02}As$ oxidation layer, and the active layer should not be etched. The mesa diameter and height are 450 $\mu$m and 5 $\mu$m respectively. The exposed $Al_{0.98}Ga_{0.02}As$ layer is laterally oxidized at 430 °C with nitrogen carrier gas bubbled through water at 85 °C. The rate of oxidation is about 1 $\mu$m min$^{-1}$ at 430 °C furnace temperature. In 25 min, a 400 $\mu$m diameter current aperture is formed, determining the active diameter of the device. After oxidation, the surface is passivated with SiN and a circular window on top of the mesa is opened for evaporating a full size p-type contact consisting of Ti–Au–Pt–Au, to provide a homogeneous current distribution and serve as a metal pad for soldering. The contact is annealed and a thick gold layer is plated over the pillar to facilitate heat sinking and future bonding. The GaAs substrate is mechanically thinned and chemically polished down to about 120 $\mu$m to decrease the substrate contribution to the series resistance, and an antireflection coating of $Si_3N_4$ with a quarter-wavelength is deposited. The $Si_3N_4$ layer is opened selectively with self-aligned reactive ion etching to evaporate an n-type Ge–Au–Ni–Au large-area electrical contact surrounding the emission windows. The whole chip is annealed at 380 °C in nitrogen environment conditions for 60 s. Finally, the device is simply soldered onto a small copper heat sink with indium solder. Neither a diamond heat spreader nor a water-cooled copper submount is used in the device packaging process.

## 3. Device performance

The device operates at room temperature (24 °C) with a pulse condition (pulse width: 50 $\mu$s; repetition rate: 1 kHz) for the testing of electrical and optical performance characteristics such as threshold current, threshold voltage, efficiency, emission wavelength, and far-field pattern.

Figure 2 shows the laser output characteristics of the device. The 400 $\mu$m diameter device has a threshold current ($I_{th}$) of 610 mA, and the maximum output power is up to 1.42 W at $I = 4$ A. The slope efficiency ($\Delta P/\Delta I$) is 0.43 W A$^{-1}$, and the wall-plug efficiency is up to 14.3%. There is no evident rollover effect in the curve due to the device heating. The threshold voltage is 1.62 V, and the differential resistance ($R_d$) is 0.13 Ω. The CW optical output power of the device is also measured at room temperature. The inset in figure 2 shows the CW optical output characteristic at room temperature, and the maximum CW optical output power is as high as 1.09 W, in the watt regime.

Figure 3 shows the measured spectrum of the device. The device emits nominally in a single mode. The peak wavelength is 987 nm, and the full width at half-maximum (FWHM) of the spectrum is 0.9 nm.

The far-field patterns of the device are plotted in figure 4(*a*). The large-area bottom-emitting device has the

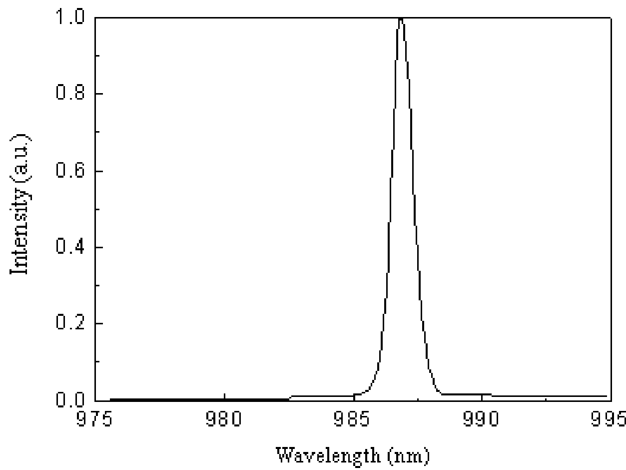


**Figure 3.** The measured lasing spectrum of the device.

intensity maximum on the symmetry axis, and no side-lobes or evident amplified spontaneous emissions are observed from the far-field patterns. The beam divergence angle is less than 10°. The lateral divergence angle $\theta_{\parallel}$ and vertical divergence angle $\theta_{\perp}$ are 9.1° and 7.9° respectively. Due to the circularly symmetric far-field patterns with low beam divergence angle the beam of the device can easily be focused or collimated into a fibre for very easy applications. For comparison, the far-field patterns of the top-emitting device is also given. Figure 4(*b*) shows the far-field patterns of a large-area top-emitting VCSEL device with the same material as the bottom-emitting device in this work. A simple change is that there is an increase in the n-type DBR period while there is a decrease in the p-type DBR period for laser top emission. The beam divergence angle of the top-emitting device is about 15°, and the lateral $\theta_{\parallel}$ and vertical $\theta_{\perp}$ are 15.3° and 16.2° respectively. The beam quality is very poor due to the serious spatial hole-burning effect from the inhomogeneous current injection through the top ring contact. Comparing figure 4(*a*) to figure 4(*b*), it is clear that the large-area top-emitting laser is not a good choice for producing an excellent high power VCSEL device structure. Therefore in this paper we put our efforts into developing a bottom-emitting VCSEL device for high power semiconductor laser use.

Why does the bottom-emitting device give a smaller divergence and different light intensity profile as compared with the top-emitting device? We attributed this, firstly, to the bottom-emitting device structure having a large-area circular n-type contact on the aperture side while the top-emitting device has a ring p-type contact; on the other hand, the p-type ring contact in the top-emitting device is nearer to the active region than the n-type large-area circular contact because of the substrate between the contact and the active region in the bottom-emitting device. Finally, the thermally induced lens effect in the transparent substrate is another important reason for the bottom-emitting device being more homogeneous.

Increasing the substrate stage temperature, the temperature characteristics of the device are also obtained in the experiment.

The variation in lasing threshold current with temperature is shown in figure 5(*a*). The temperature varies from 0 °C to 100 °C. The threshold current is minimized for temperatures between 20 °C and 30 °C. For a lower temperature or a higher temperature, the threshold current increases with temperature. The threshold current decreases monotonically with increasing heat stage temperature in the low temperature range from 0 °C to 20 °C due to the negative gain–cavity offset. The threshold current increases monotonically with increasing heat stage temperature in the high temperature range from 30 °C to 100 °C due to the positive gain–cavity offset. This

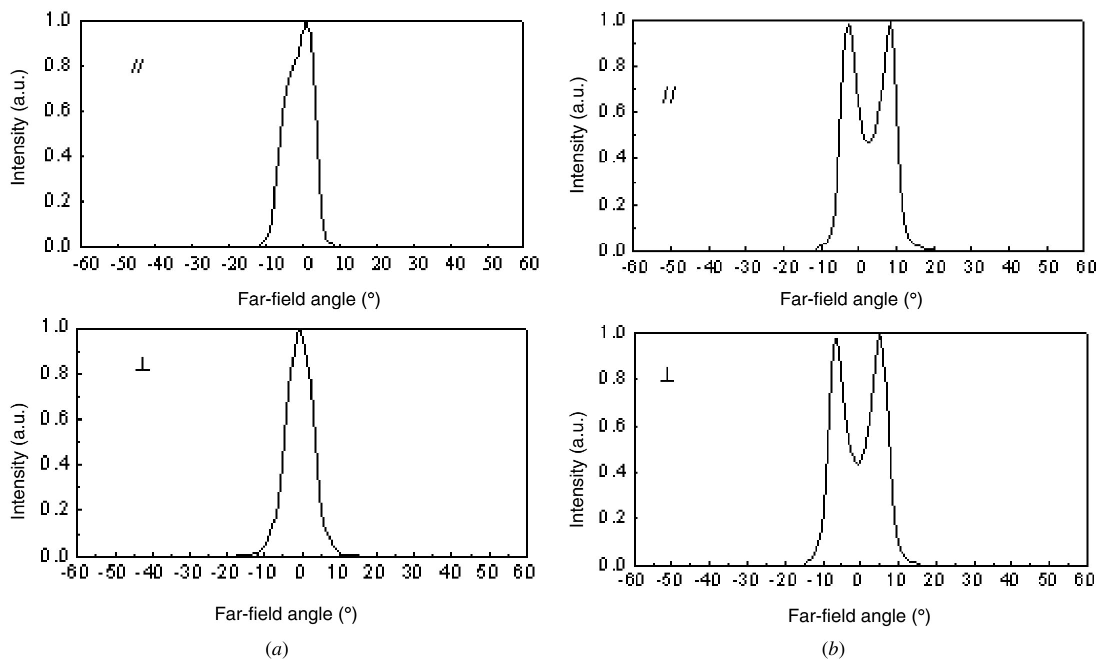


**Figure 4.** (*a*) Measured far-field patterns of the bottom-emitting device. (*b*) Measured far-field patterns of the top-emitting device.

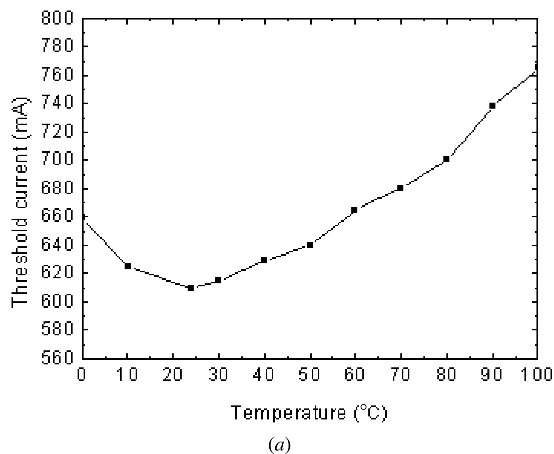


(*a*)

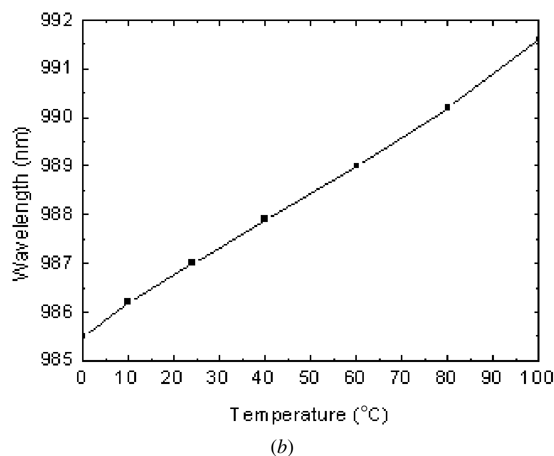


(*b*)

**Figure 5.** (*a*) The measured temperature dependence of the threshold current. (*b*) The measured temperature dependence of the lasing peak wavelength.

is a special temperature dependence of the threshold current due to the gain–cavity offset in the VCSEL structure. The special behaviour is due to the diversity between the temperature dependence of the material gain peak and the cavity resonance, and the material gain peak red-shifting at a higher rate than the Fabry–Perot mode as the temperature increases. The gain–cavity offset of the structure at room temperature used in this paper is selected as the zero offset. By changing the negative or positive offset, the minimum threshold current can be selected in lower or higher temperature conditions for temperature sensitive operation. By using the characteristic temperature function $I_{th} = I_0 \exp\left(\frac{T}{T_0}\right)$ from the literature [15], where $I_0$ is a constant, the characteristic temperature $T_0$ of the device is derived. The value is over 220 K. Such a high characteristic temperature of the threshold current can lead to good temperature sensitivity of the device.

At the same time, the lasing spectrum characteristics with varying temperature are also measured. The experimental temperature dependence of the lasing peak wavelength is shown in figure 5(*b*), and the wavelength shift with temperature is about 0.06 nm $K^{-1}$. The lasing peak wavelength is the cavity resonance in a VCSEL structure, so it is increased monotonically with temperature as $\lambda = \lambda_0 + mT$ with $m = 0.06$ nm $K^{-1}$ in the device. Figure 6 shows the laser spectrum

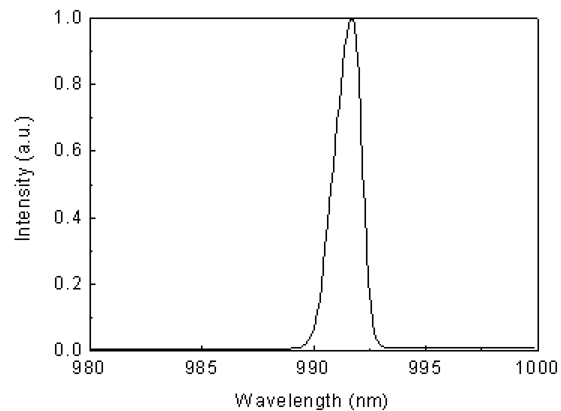


**Figure 6.** The measured lasing spectrum of the device at 100 °C.

at the temperature of 100 °C. It is apparent that even at high temperature the device emits nominally in a single mode, there is no evident distortion, and the FWHM of the spectrum is spread to 1.4 nm at 100 °C.

## 4. Conclusion

In summary, we have reported the fabrication and performance characteristics of a high (watt-level) power oxide-confined bottom-emitting InGaAs/GaAsP VCSEL with large aperture. The device with 400 $\mu$m diameter operates at room temperature with a pulse condition (pulse width: 50 $\mu$s; repetition rate: 1 kHz). The threshold current is 610 mA, and the maximum output power is up to 1.42 W with a wall-plug efficiency of 14.3% at a single wavelength. The maximum continuous wave (CW) optical output power at room temperature is as high as 1.09 W. So both the pulse condition and the CW maximum optical output power are up to the watt regime. The lasing peak wavelength is 987 nm, and the full width at half-maximum (FWHM) is 0.9 nm. The far-field divergence angles, lateral $\theta_{\parallel}$ and vertical $\theta_{\perp}$ are 9.1° and 7.9° respectively, and the laser has a circular light beam and the intensity maximum on the symmetry axis from the measured far-field patterns. Increasing the substrate stage temperature, the dependence of the threshold current on the temperature is obtained experimentally. The threshold current is minimized for a temperature between 20 °C and 30 °C. By changing the negative or positive gain–cavity offset, the minimum threshold current can be selected in lower or higher temperature conditions for temperature insensitive operation, and the special behaviour may also be used as a factor for judging the device structure and epitaxy quality for optimizing the device structure design and materials growth in VCSEL fabrication. The characteristic temperature $T_0$ of the device is over 220 K. Such a high characteristic temperature of the threshold current can lead to good temperature sensitivity. The wavelength change of the device with temperature is also studied, and the wavelength shift with temperature is just about 0.06 nm $K^{-1}$.

## Acknowledgments

This work is supported by the Academic Excellence program of Changchun Institute of Optics, Fine Mechanics, and

Physics, Chinese Academy of Sciences and by the National Science Council of the Republic of China under contract numbers 10104016, 60306004.

## References


[1] Wiedenmann D, King R, Jung C, Jager R and Michalzik R 1999 Design and analysis of single-mode oxidized VCSEL's for high-speed optical interconnects *IEEE J. Sel. Top. Quantum Electron.* **5** 503–11

[2] Geels R S, Corzine S W and Coldren L A 1991 InGaAs vertical cavity surface emitting lasers *IEEE J. Quantum Electron.* **27** 1359–67

[3] Mederer F, Jager R, Schnitzer P, Unold H, Kicherer M, Ebeling K J, Natomi M and Yoshida R 2000 Multi-Gigabit/s graded-index POF data link with butt-coupled single-mode InGaAs VCSEL *IEEE Photonics Technol. Lett.* **12** 199–201

[4] Weigl B, Grabherr M, Jung C, Jager R, Reiner G, Michalzik R, Sowada D and Ebeling K J 1997 High-performance oxide-confined GaAs VCSELs *IEEE J. Sel. Top. Quantum Electron.* **3** 409–15

[5] Jäger R, Grabherr M, Jung C, Michalzik R, Reiner G, Weigl B and Ebeling K J 1997 57% wallplug efficiency oxide-confined 850 nm wavelength GaAs VCSEL's *Electron. Lett.* **33** 330–1

[6] Ueki N, Nakayama H, Sakurai J, Murakami A, Otoma H, Miyamoto Y, Yamamoto M, Ishii R, Yoshikama M and Nakamura T 2001 Complete polarization control of 12 × 8-Bit matrix-addressed oxide-confined vertical-cavity surface-emitting laser array *Japan. J. Appl. Phys.* **40** L33–5

[7] Amann M C, Ortsiefer M, Shau R and Robkopf J 2002 Vertical-cavity surface-emitting laser diodes for telecommunication wavelengths *Proc. SPIE* **4871** 123–9

[8] Lan Y P, Chen Y-F, Huang K F, Lai H C and Pan J S 2002 Oxide-confined vertical-cavity surface-emitting lasers pumped Nd: YVO4 microchip lasers *IEEE Photonics Technol. Lett.* **14** 272–4

[9] Wu J, Lordache G, Summers H D and Roberts J S 2001 Optical characteristics of VCSEL pumped microchip lasers *Opt. Commun.* **196** 251–6

[10] Gibson G M, Conroy R S, Kemp A J, Sinclair B D, Padgett M J and Dunn M H 1998 Microchip laser-pumped continuous-wave doubly resonant optical parametric oscillator *Opt. Lett.* **23** 517–8

[11] Chang C H, Earles T and Botez D 2000 High CW power narrow-spectral width 980 nm broad-stripe distributed-feedback diodes lasers *Electron. Lett.* **36** 954–5

[12] Bouwmans G, Percival R M, Wadsworth W J, Knight J C and St J Russell P 2003 High-power Er:Yb fiber laser with very high numerical aperture pump-cladding waveguide *Appl. Phys. Lett.* **83** 817–8

[13] Miller M, Grabherr M, King R, Jäger R, Michalzik R and Ebeling K J 2001 Improved output performance of high-power VCSELs *IEEE J. Sel. Top. Quantum Electron.* **7** 210–6

[14] Grabherr M, Jäger R, Miller M, Thalmaier C, Heerlein J, Michalzik R and Ebeling K J 1998 Bottom-emitting VCSEL's for high-CW optical output power *IEEE Photonics Technol. Lett.* **8** 1061–3

[15] Agrawal G P and Dutta N K 1993 *Semiconductor Lasers* (New York: Van Nostrand-Reinhold) pp 6–130